Scientific journal of Research studies in Future Computer Sciences, 2024, Vol. 1, No. 1, pp. 1-12

Scientific journal of Research studies
in Future Computer Sciences
www.journalhi.com/com/

Optical Binary Adder Gate modeling using optical digital IC

Saeed Maddahi Kivi * 1

1- Optical Telecommunications group, Electrical and Computer college, University of Tabriz, Tabriz, Iran.
* saeedmaddahikivi@gmail.com

Article Information

Original Research Paper
Received
Accepted
Available

Keywords:
Simulation
OR Logical Gate
Circular resonator
Integrated Circuits
Digital

Abstract

Logic devices and gates perform an essential part in modern electronics and integrated circuits. Recently, all optical logic gates in addressing, switching, encryption, data encryption, signal reconstruction, have given significant importance in their applications in optical communication networks. In recent years, various designs have been introduced for the design of all optical logic gates based on linear light effects, such as interference, semiconductor optical amplifier (SOA), and Mach Zehnder interferometer (MZI) and processes. Logic gateways are capable of performing many logical functions and have numerous applications in optical communications such as logic gateways for address recognition, correction and data integrity verification, and are also used as a sampling gateway in optical sampling oscilloscopes. In this paper, all the designs are based on triangular two-dimensional simulations. In the proposed design, a ring consisting of several waveguides and port A and port B are considered as inputs. The output leaves the structure through the output waveguide. To design logic gates, we calculate all the optical transitions for the desired structure for the possible modes for the OR logic gate. Then, by selecting the optimal point for a / λ and considering λ = 1.55 μm, we design the logical gate of the idea. By applying the radius in the previous step and simulating the structure of the electromagnetic field distribution, we obtain the part. Which indicates the realization of the desired gate.

1- Introduction

Although the study of optical crystals began in 1887, the term optical crystals was first used a hundred years later, in 1987 by Eli Yablonovich and John when they published two important papers on photonic history on optical crystals. Took [1]. Before 1987, one-dimensional optical crystals were studied in detail as multilayer periodic masses such as Bragg mirrors [2]. Lord Riley started his studies in 1887 by showing that these structures have a one-dimensional bandgap, a spectral range of high reflectivity known as the stop band [3]. Today, such bands have been used in a variety of applications. From high-reflectance coating layers to increase diode efficiencies to high-reflectance mirrors in laser cavities. For example, VCSEL is a detailed study. Theoretical theory of optical crystals was developed by Vladimir Bykov, who studied the effect of the Gap band on the spontaneous emission of atoms and molecules [4]. Bykov also thought about what might happen if alternating two- and three-dimensional structures were used. However, the concept of three-dimensional optical crystals was explored in 1979 by Ohtaka, who proposed a method for calculating the Gap band photonics [5]. However, these ideas did not flourish until the publication of Yablunovich and Jan's paper. Both papers were involved with high-dimensional optical crystals. Yablonovich's main motivation was to engineer the density of photonic states to control spontaneous emission within optical crystals. The idea of using optical crystals to influence the motion of photons and trap them Was. After 1987, the number of research papers on optical crystals grew exponentially [6]. Despite these difficulties in making optical crystals, further studies in the field of theory or in practice are limited to the micrometer regime. Optical crystals can easily be made in centimeters. Which worked in micrometer mode. The structure that Yablonovich succeeded in constructing was in fact a number of perforated arrays within a transparent environment. That the holes in each structural layer created the diamond image. They are known today as Yablonovit. In 1996, Thomas Krauss introduced the first two-dimensional optical crystal structure in the visible light range [7]. This opened up a new way for optical crystals to use semiconductor materials in construction, as they do in the semiconductor industry. Today, these techniques use optical crystal blades. These blades are actually two-dimensional optical crystals printed on semiconductor blades. The general reflection traps light inside the blade, allowing the effects of optical crystals such as photonic diffraction engineering to occur inside the blade. Research is underway around the world to use optical crystals in computer circuits. To improve the analysis of optical communications within and between chips. Although these applications are considered as a commercial application, 2D optical crystals in the form of optical crystal fibers have been widely used. The study of three-dimensional optical crystals was progressing at a much slower rate than two-dimensional optical crystals. This was due to the many problems in making this type of optical crystal. Three-dimensionality had not inherited any simplicity from the semiconductor industry in the simplicity of construction and production methods. Has made. Another set of efforts to make 3D optical crystals in the field of its own crystals. The basis of this method is the production of immersion of a nanometer dielectric sphere in a solution with a three-dimensional periodic structure that has a gap band. The first example of this was done in 2000 at the University of Toronto, Canada. The new field to better understand these structures was the study of living organisms, which in 2006 led researchers to a natural optical crystal the size of a Brazilian beetle [4]. Optical crystals have many applications in optical electronics. One of these applications is the construction of optical gates by two-dimensional optical crystals, which is used today as a new method in the construction of optical gates. The advantages of these optical gates are simple structure, high speed and low power consumption. For this reason, these optical gates can be used instead of electronic gates. Before discussing the optical gates, we first discuss the two-dimensional structures of the optical gates, then we will avoid the optical gates, and also mention some examples of optical gates that are completely similar to the similar ones. We will pay for the construction . The basis of this method is the production of immersion of a nanometer dielectric sphere in a solution with a three-dimensional periodic structure that has a gap band. The first example of this was done in 2000 at the University of Toronto, Canada. The new field to better understand these structures was the study of living organisms, which in 2006 led researchers to a natural optical crystal the size of a Brazilian beetle [5]. Graphene has become a unique material due to its extraordinary properties in electrical conductivity and thermal conductivity, high density and mobility of load carriers, optical conductivity [7] and mechanical properties [8] Due to these mechanical properties. this new solid-state system is considered as a very suitable candidate to replace silicon in the next generation of photonic and electronic components, and therefore has attracted little background in basic and applied research. Due to the fact that graphene is an intermediate material that can be used in both electronics and photonics. Therefore, there is also attention to the construction of opto–electronic logic gates [9-10]. And in many active devices such as logic gate and filter [11] modulator [12,13], switches [14], etc. have been used. Optical logic gates are essential devices for the processing of optical signals. They are based on many different structures, such as semiconductor optical amplifiers [15-17] are designed for photon crystals [18-20], plasmonic waveguides [22-21] and so on. However, the above structures have their own problems. Authors in [23] A method for designing a plasmon waveguide based on graphene with They presented low wavelengths that act as a switch or a logic gate, and a few years later reported that logic valves were reported to use constructive and destructive interference between graphene- plasmon waveguide based on graphene [24] Optical logic gates based on fiber have the problem of chip-scale integration. Optical logic gates based on waveguide interferometers have a complex structural arrangement. Also, such gates are limited by momentary emission noise due to the structure of microsonductors and semiconductor optical amplifiers [25].The presence of photonic crystals in the design of optical logic gates has created a high potential for compaction and reduction of the size of ultra-fast switching components and reduction of power consumption [26] Wavelength limit used [27] Photonic crystals selectively reflect or transmit light at different wavelengths. There is a range of wavelengths in the crystal that completely reflects light due to the rotation of the crystal lattice, and that range is called the photonic Band gap (PBG). Let us guide. The defect is caused by removing a row of rods in the structure of the crystal lattice, which is called the waveguide [28].An all-optical photonic crystal logic gate has been proposed in which two right waveguides and a photonic resonator

located between the two waveguides are used to form the logic gate used between the waveguides. The resonator is located at an angle of 45 degrees between the waveguides, which at some frequencies leads to destructive interference and makes the power transmission operation difficult. The transfer rate in LOW mode is 17% and the transfer rate in HIGH mode is 85%. [29] .In [30] they proposed the design of two all-photonic logic gates, one of which was the NOT gate. In the structure of this gate, two right photonic waveguides are used Crossing. In the center of this logical gate, a non-linear rod with a larger radius than the other rods is used, which increases the power consumption gate. The amount of power transfer at the logic gate output Logically, 90% is reported in the active state.The authors [31] have proposed another all-optical logic gate design. In this design, the photonic crystal structure with a triangular network of air holes in the substrate of the dielectric material is used. Optical crystals have many applications in optical electronics. One of these applications is the construction of optical gates by two-dimensional optical crystals, which is used today as a new method in the construction of optical gates. The advantages of these optical gates are simple structure, high speed and low power consumption. For this reason, these optical gates can be used instead of electronic gates. Before discussing the optical gates, we first discuss the two-dimensional structures of the optical gates, then we will avoid the optical gates, and also mention some examples of optical gates that are completely similar to the similar ones. We will pay for the construction

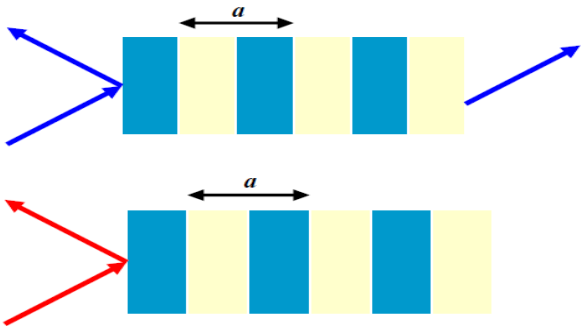

Figure 1. One-dimensional photon crystal and its response to two different wavelengths [20-21]

It is called a network constant or periodicity and represents the minimum length of space in which the network structure is repeated. In other words (ε (x) = ε (x + a) in which (x) ε is a spatial function of electrical conductivity. These areas are called photon gaps or frequency bands. Between two consecutive photon gaps, there is an allowable frequency band (and vice versa) in which wave propagation is possible under certain conditions. If a photonic gap with a frequency interval [f1, f2] is specified where f1> f2 then fc = (f1 + f2) / 2 the central frequency of the gap Δfc = f1-f2 is called the bandwidth. Let us now briefly consider the equations governing optical crystals. Maxwell equations in alternating environments:

$$\left.\begin{aligned}\nabla\times\vec{E}&=-\frac{\partial\vec{B}}{\partial t}\\ \nabla\times\vec{H}&=-\frac{\partial\vec{D}}{\partial t}+J\\ \nabla\cdot\vec{D}&=\rho\\ \nabla\cdot\vec{B}&=0\end{aligned}\right\} \quad (1)$$

For an environment without free charge and free electric current density where the conditions $\rho(r)=0$, $J(r)=0$ prevail, the Maxwell equations are simplified and in fact linear as follows:

$$\left.\begin{aligned}\nabla\times\vec{E}&=-\frac{\partial\vec{B}}{\partial t}\\ \nabla\times\vec{H}&=\frac{\partial\vec{D}}{\partial t}+J\\ \nabla\cdot\vec{D}&=0\\ \nabla\cdot\vec{B}&=0\end{aligned}\right\} \quad (2)$$

For a system that is in the state of sinusoidal and single frequency, it is appropriate to analyze the electric and magnetic fields by phasors:

$$\left.\begin{aligned}\vec{E}(r,t)&=\mathrm{Re}[E(r)e^{j\omega t}]\\ \vec{D}(r,t)&=\mathrm{Re}[D(r)e^{j\omega t}]\\ \vec{B}(r,t)&=\mathrm{Re}[B(r)e^{j\omega t}]\\ \vec{H}(r,t)&=\mathrm{Re}[H(r)e^{j\omega t}]\end{aligned}\right\} \quad (3)$$

Where ω is the source frequency. Therefore, Maxwell equations in the mixed space of phasors appear as follows:

$$\left.\begin{aligned}\nabla\times\vec{E}&=-j\omega\mu_0 H\\ \nabla\times\vec{H}&=j\varepsilon(r)\omega E\\ \nabla\cdot D&=0\\ \nabla\cdot B&=0\end{aligned}\right\} \quad (4)$$

Given that we have zero divergence of B vectors $\nabla\cdot H=0$. But the divergence of field E will appear as follows:

$$\nabla\cdot D=\nabla\cdot(\varepsilon E)=\varepsilon\nabla\cdot E+\nabla\varepsilon\cdot E=0 \quad (5)$$

So you get:

$$\nabla\cdot E=-\frac{\nabla\varepsilon}{\varepsilon}\cdot E=\nabla\ln\varepsilon\cdot E\neq 0 \quad (6)$$

$$c=\frac{1}{\sqrt{\mu_0\varepsilon_0}}$$

Finally, using the previous equations, we will reach the following equations.

Equations governing optical crystals

$$\left.\begin{aligned}\frac{1}{\varepsilon_r}\nabla\times\nabla\times E=\frac{\omega^2}{c^2}E\\ \nabla\times\left(\frac{1}{\varepsilon_r}\nabla\times H\right)=\frac{\omega^2}{c^2}H\end{aligned}\right\} \quad (7)$$

We define it as follows: L_E, L_H Now two operators

$$L_E=\frac{1}{\varepsilon_r}\nabla\times\nabla(E) \quad (8)$$

$$L_H=\nabla\times\left(\frac{1}{\varepsilon_r}\nabla\times(H)\right) \quad (9)$$

As a result, the special equation for the amount of electric and magnetic fields appears as follows:

$$\left.\begin{aligned}L_E E=\frac{\omega^2}{c^2}E\\ L_H H=\frac{\omega^2}{c^2}H\end{aligned}\right\} \quad (10)$$

It should be noted that in fact to obtain electric and magnetic fields it is not necessary to solve both equations, but it is enough to solve one of them and use Maxwell's equations to obtain the other. But in one-dimensional and two-dimensional problems, one of the equations (10) is usually in the form of simple fences and it becomes much easier to solve. However, depending on the quantity of fences, electrical or magnetic polarization is analyzed. It can also be shown that L_H in principle pragmatism is self-contained, while this L_E is not necessarily the case. We will now briefly discuss the solution of Maxwell equations in one-dimensional and two-dimensional optical crystals. Consider a one-dimensional photonic crystal as follows.

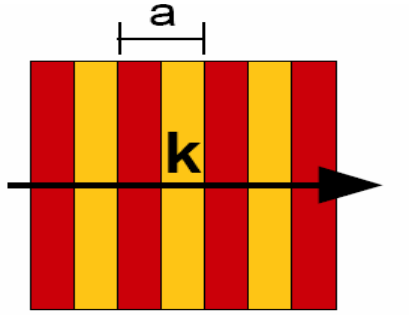

Figure 2. One-dimensional photonic crystal [20-21].

According to TE, TM modes as follows:

$$\left.\begin{aligned}L_E E=\frac{\omega^2}{c^2}E\\ L_H H=\frac{\omega^2}{c^2}H\end{aligned}\right\} \quad (11)$$

Now according to the following relation

$$\nabla\times\nabla\times A=\nabla(\nabla.A)-\nabla^2 A \quad (12)$$

And using relation (6) and (7) we have

$$\nabla\times\nabla\times A=\nabla(\nabla.A)-\nabla^2 A \quad (13)$$

If the electric field does not have an x component then:

$$\nabla\times\nabla\times A=\nabla(\nabla.A)-\nabla^2 A \quad (14)$$

So:

$$\left\{\begin{aligned}-\left[\frac{\partial^2}{\partial x^2}+\frac{\partial^2}{\partial y^2}+\frac{\partial^2}{\partial z^2}\right]E_y(x,y,z)=k_0{}^2\varepsilon_r(x)E_y(x,y,z)\\ -\left[\frac{\partial^2}{\partial x^2}+\frac{\partial^2}{\partial y^2}+\frac{\partial^2}{\partial z^2}\right]E_z(x,y,z)=k_0{}^2\varepsilon_r(x)E_z(x,y,z)\end{aligned}\right. \quad (15)$$

Here with the help of Fourier transform to y and z as:

$$A_i(x;y,z)=\frac{1}{(2\pi)^2}\iint E_i(x;y,z)e^{j\beta y}e^{j\gamma z}dydz, \quad \text{i=y,z} \quad (16)$$

The components of the electric field are written as follows:

$$E_i(x;y,z)=\iint A_i(x;\beta,\gamma)e^{-j\beta y}e^{-j\gamma z}dydz, \quad \text{i=y,z}$$

Now considering the derivative relations (17)

$$\frac{\partial}{\partial y}\to -j\beta,\frac{\partial}{\partial z}\to -j\gamma$$

$$-\left[\frac{\partial^2}{\partial x^2}+(\beta^2+\gamma^2)\right]A_i(x,y,z)=k_0{}^2\varepsilon_r(x)A_i(x,y,z);\ \text{i=y,z} \quad (18)$$

If $\gamma=0$ so:

$$\frac{\partial^2 A(x)}{\partial x^2}+k^2(x)A(x)=0;\quad k^2(x)=[k_0{}^2\varepsilon_r(x)-\beta^2] \quad (19)$$

By solving the above equation by the approximate

It will be slow, $k^2(x)$ WKB method if the changes we will have:

$$A(x)\cong c_1\exp[-j\int_{x_0}^{x}k(x')dx']+c_2\exp[+j\int_{x_0}^{x}k(x')dx$$

$$A(x)\cong c_1\exp[-jk(x)]+c_2\exp[+jk(x)] \quad (20)$$

(21)

In this way we will have a one-dimensional: optical crystal

$$a\ permitive\ \text{cell:}0<x<X \rightarrow \varepsilon=\varepsilon_1 \ \wp\ X<x<L \rightarrow \varepsilon=\varepsilon_2$$

$$Where\ \ \varepsilon=\varepsilon_1:$$

$$A_1(x)=a_1^+e^{-jK_1x}+a_1^-e^{+jK_1x}$$

$$Where\ \ \varepsilon=\varepsilon_2:$$

$$A_2(x)=a_2^+e^{-jK_2x}+a_1^-e^{+jK_2x}$$

Given that the tangential component continuity of the fields E, H will lead to the self- function and derivative continuity in the discontinuous loci ,we will have:

$$\begin{bmatrix}a_2^+\\a_2^-\end{bmatrix}=\frac{1}{-2}K_2\begin{bmatrix}-K_2e^{jK_2X} & -e^{-jK_2X}\\-K_2e^{-jK_2X} & e^{-jK_2X}\end{bmatrix}\begin{bmatrix}e^{-jK_1X} & e^{jK_1X}\\K_1e^{-jK_1X} & -K_1e^{jK_1X}\end{bmatrix}\begin{bmatrix}a_1^+\\a_1^-\end{bmatrix} \quad (22)$$

On the other hand, given that the answers must be true in terms of Blah's theory, we will have

$$\left.\begin{aligned}\phi_k(x)=\psi(x)e^{jkx}=\phi_k(x+L)\\ \psi_1(x)e^{jkx}=\phi_2(x+L)e^{jk(x+L)}\end{aligned}\right\} \quad (23)$$

Therefore:

$$\begin{bmatrix}a_1^+\\a_1^-\end{bmatrix}=\begin{bmatrix}e^{jkL}e^{-j(K_2-K_1)X} & 0\\0 & e^{jkL}e^{j(K_2-K_1)X}\end{bmatrix}\begin{bmatrix}a_2^+\\a_2^-\end{bmatrix} \quad (24)$$

Using equations (13) and (14) we will have:

$$\begin{bmatrix}a_2^+\\a_2^-\end{bmatrix}=\frac{1}{-2}K_2\begin{bmatrix}-K_2e^{jK.X} & -e^{-jK.X}\\-K_2e^{-jK.X} & e^{-jK.X}\end{bmatrix}\begin{bmatrix}e^{-jK.X} & e^{jK.X}\\K_1e^{-jK.X} & -K_1e^{jK.X}\end{bmatrix}\begin{bmatrix}e^{jkL}e^{-j(K_2-K_1)X} & 0\\0 & e^{jkL}e^{j(K_2-K_1)X}\end{bmatrix}\begin{bmatrix}a_2^+\\a_2^-\end{bmatrix}$$

$$\rightarrow\frac{1}{-2}K_2\begin{bmatrix}-K_2e^{jK.X} & -e^{-jK.X}\\-K_2e^{-jK.X} & e^{-jK.X}\end{bmatrix}\begin{bmatrix}e^{-jK.X} & e^{jK.X}\\K_1e^{-jK.X} & -K_1e^{jK.X}\end{bmatrix}\begin{bmatrix}e^{jkL}e^{-j(K_2-K_1)X} & 0\\0 & e^{jkL}e^{j(K_2-K_1)X}\end{bmatrix}$$

$$\text{if } Q=\frac{1}{-2}K_2\begin{bmatrix}-K_2e^{jK.X} & -e^{-jK.X}\\-K_2e^{-jK.X} & e^{-jK.X}\end{bmatrix}\begin{bmatrix}e^{-jK.X} & e^{jK.X}\\K_1e^{-jK.X} & -K_1e^{jK.X}\end{bmatrix}$$

$$Q=\begin{bmatrix}q_{11} & q_{12}\\q_{21} & q_{22}\end{bmatrix}$$

$$\rightarrow\cos(kL)=\frac{q_{11}+q_{22}}{2}\cos(KL)-j\frac{q_{11}-q_{22}}{2}\sin(kL) \quad (25)$$

Equation (15) is called the scattering equation. In fact q_{ii}, they are in the diagonal layers Q, they are $K_i=K_i(\omega;\beta)$ self-dependent and are a function of the frequency and constant propagation. Now with a fixed assumption (for example) the right side of Equation (24) can be represented by a function such as :

$$\cos(kL)=f(\omega) \quad (26)$$

According to Equation (25), the following three cases can be considered:

$$\left.\begin{aligned}|f(\omega)|<1 \rightarrow k\in R,\ \mathrm{Im}[k]=0\\ f(\omega)=\pm1 \rightarrow k=m\frac{\pi}{L},\ m\in Z\\ |f(\omega)|>1 \rightarrow k\in R,\ \mathrm{Re}[k]=m\frac{\pi}{L},\mathrm{Im}[k]\neq0\end{aligned}\right\} \quad (27)$$

Given that it is a $f(\omega)$ continuous function of frequency, it can be concluded that there are also continuous intervals in the $|f|>1,|f|\leq1$ neighborhood in which it is. The permissible band is frequency for the interval of the first type in which the real and its blue waves have a limited amplitude, and for the interval of the second type in which the imaginary and its blue waves have an infinite amplitude on one side, the band is frequency prohibited. Or photon gap. In a photonic gap, it is not possible to propagate a wave in a photonic crystal, and if the width of the crystal is limited, the transmittance will be very small.

2- Introduction of RSOFT software

The software used in this paper that is used to simulate optical crystals is RSOFT software. The basis of this software is Maxwell equations, which are solved numerically and programmed in software. An important advantage of this software is its graphical environment and it is also dedicated to the analysis of optical crystals. In this paper, the desired software is used to obtain the photon band and also the distribution of the electric field in the photon crystal.

Optical gates designed using two-dimensional optical crystals

2-1- Optical gates designed using Mach Zehnder's optical crystal waveguide

These types of gates are made using Mach Zehnder filter, which consists of two-dimensional optical crystals with a triangular lattice. The structure of this gate is shown in Figure (3) [1].

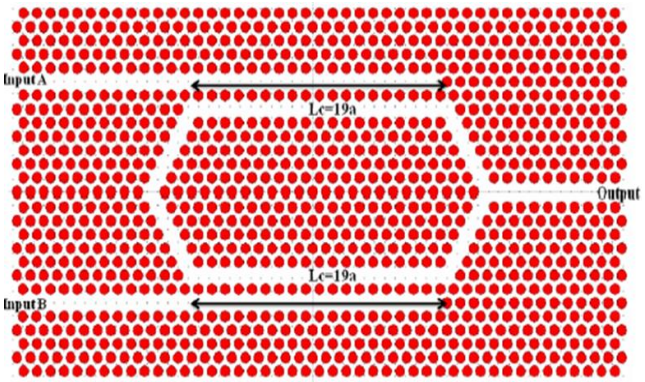

Figure 3. Mach Zehnder optical gate structure

The structure consists of a photonic crystal with a triangular lattice and dielectric rods in the air, which have a dielectric constant of n = 3. 4 (ε = 11. 56) and bar radius r = 0. 35a (a: network constant). Using the PWE method, the photon band is calculated as shown in Figure (16). The component structure consists of two input ports and one output port. In this simulation the input electric field wavelength = 1. 55μm λ and the length of the arms of this filter is 19a.

In this paper, all designs are based on triangular two-dimensional simulations. The two-dimensional photonic crystal structure, as shown in Figure 1, consists of a triangular lattice 21a×21a consisting of air holes in silicon with a refractive index of n = 3.46. The radius of air is r = 0.35a and a is the lattice constant of the structure, which is equal to a = 0.674 μm.

In the proposed scheme, 4 waveguides have been created that port A and port B are considered as inputs. As shown in Figure 4, the output signals are obtained from the right port shown as the OUT output port.

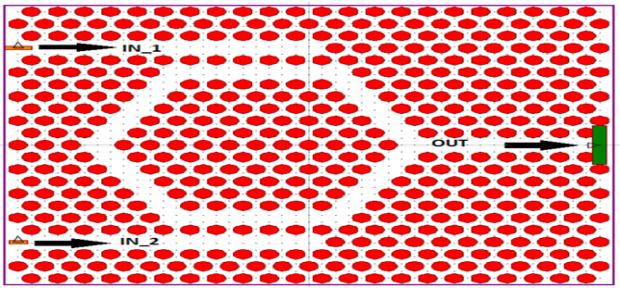

Figure 4. View of the all-light gate.

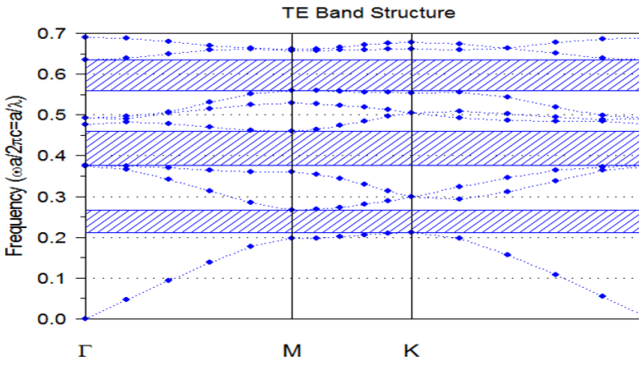

Figure 5. Introduced crystal photonic band structure.

The TE optical band structure is shown in the figure above. This figure is calculated using the PWE method in the RSOFT software called the Bandstructure section.

As you know, the second forbidden band is in the range. By selecting the appropriate a, the function of the part can be designed in the telecommunication wavelength window. Here, the radius is considered to be a = 0.674 μm, in which case the first forbidden band will be in the range, resulting in a window of 1.55 μm telecommunication wavelength. The correct table of the OR logic gate is as follows.

Table 1. Logical operation of NAND gate

Input A	Input B	Output O
0	0	0
0	1	1
1	0	1
1	1	1

In all-optical mode, that is, when the input signals, whether reference or A and B, are in the form of Gaussian light waves with intensity and fit and without phase difference from each other.

To design the desired OR gate, the output spectrum must be obtained for the given inputs. The following figures show the output bands in the output port for the two input modes given.

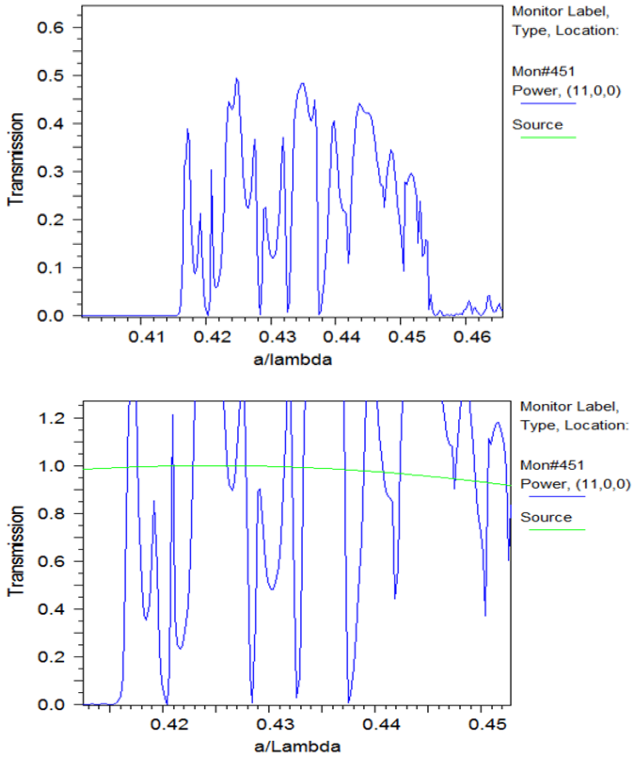

Figure 6. Transit output spectrum diagram for a) A = 1, B = 0 and b) A = 1, B = 1

As shown in Figure 7, by selecting the appropriate point, the OR logic gate can be designed to fit the given table correctly. In the diagram above, in order to obtain the transmission spectrum, in the RSOF software, the FDTD part of the inputs must be applied to the structure in the form of a pulse in order to obtain the output spectrum or frequency response. In Figure 5, if we select a point, then in state A (where both inputs are A = B = 0) then T = 0.5, which corresponds to a logic. In case B (case where both inputs are A = 1, B = 1) then T = 1.9, which corresponds to a logic.

Thus, it is possible to design an all-optical OR logic gate with 1 logic corresponding to a power between 0.5P0 to 2P0 and also a logic zero with a power less than 0.1P0.

By selecting the appropriate wavelength, the desired frequency can be calculated according to. The results of gate simulation with input wavelength as well as network radius with RSOFT software FDTD section are as follows.

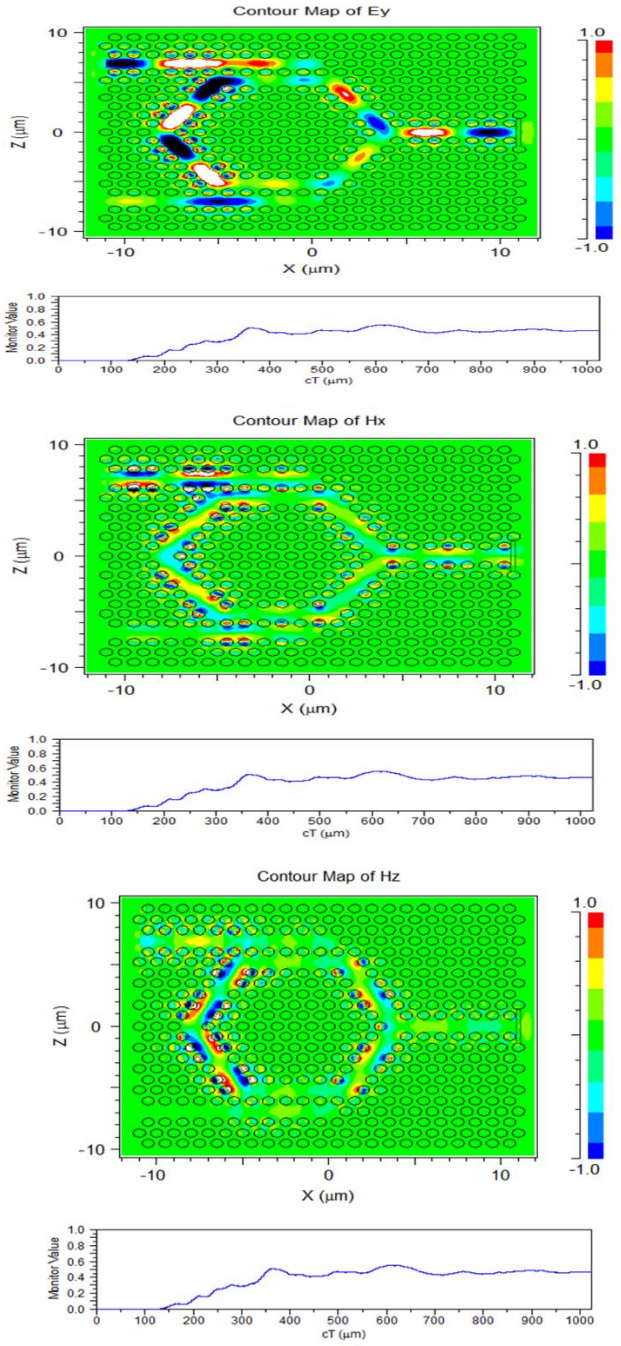

Figure 7. Distribution of magnetic field from top to bottom Ey, Hx and Hz in two dimensions, respectively, with a graph of passage in time for A = 1, B = 0, which do not differ in time phase.

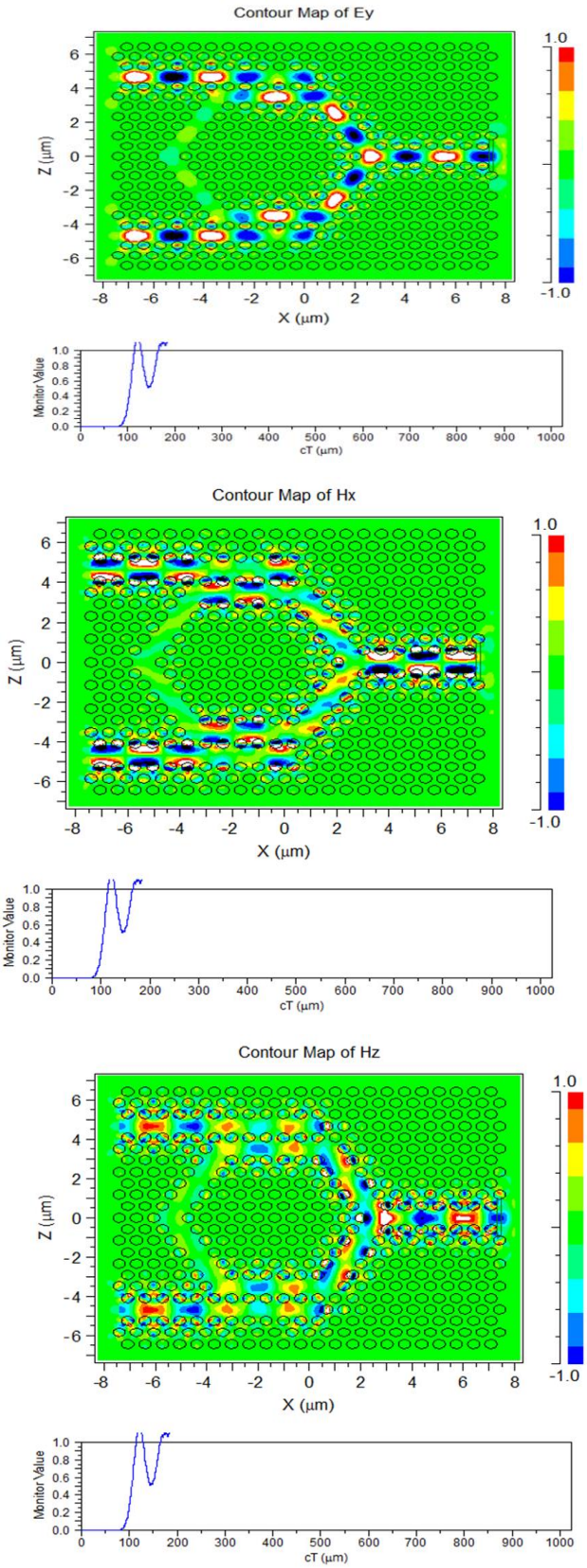

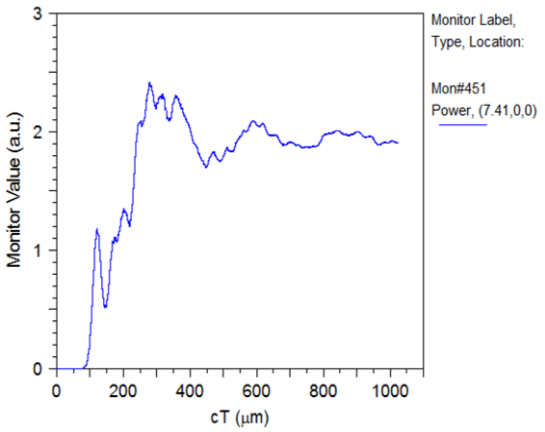

Figure 8. Distribution of the magnetic field from top to bottom Ey, Hx and Hz in two dimensions, respectively, with a passage diagram in terms of time for A = 1, B = 1 that do not differ in time phase. The last diagram also shows the passage for the high dampers.

According to the simulations performed, the results indicate an all-optical component with OR function. The function table of the part is given below.

Table 2. Optical function table of OR gate

Input A	Input B	Logical output	Optical power at the output
0	0	0	0
0	1	1	0.5 P_0
1	0	1	0.5 P_0
1	1	1	2 P_0

3- Conclusion

According to the simulations performed, the all-optical OR logic gate was designed and simulated. This gate is set at a wavelength of 1.55 .m telecommunication window. Because in fiber optic communications, the set wavelength is usually this wavelength. Depending on the design, the adjusted wavelength structure can be changed to, for example, 1.33 µm by changing the periodicity. The simulated part is all light, which means that only light is emitted in the part. The structure of the piece is also very simple and includes dielectrics made of glass, which are very common in nature. In this simulation, two inputs A and B are entered into the system without phase difference. The correct operation of the piece at the desired wavelength is based on constructive and destructive interference. According to the design and simulation, the logic zero for the optical power component is less than 0.1 P0 and a logic optical power greater than 0.4 P0, P0 is the input light power. According to the simulations, the steady state of the part occurs at CT = 300µm, where C is the speed of light in a vacuum and T is the period of rotation when the frequency inverse or the same bit per second. So the frequency of the piece is 1THz or 1 Tbit / sec. Which is very fast and is also a good component for all-optical digital processing circuits.

and different temperatures. Also, Nakamura and his colleagues [3] have investigated the effect of temperature difference in creating immersion movements in fluid. In their research, they have predicted changes in fluid flow by using Bozinsk approximation and numerical solution of Navier-Stokes equations and have investigated the rate of heat transfer from the fluid caused by free movement.

4- Conclusions

In the last two decades, due to its many applications, researchers have paid much attention to free movement. One of these applications is in the cooling of electronic equipment. Temperature control of the internal parts of these devices is one of the important parameters in their design and construction. The heat produced in these parts can be transferred outside the device in the form of free movement. Examples of such equipment include microprocessors, ICs, and heat generating parts in portable computers, remote communication equipment, and many electronic equipments that are locked in the space of the device. Among the early accurate works in the field of free movement, we can mention the studies of Saito and Harris [1], and Duhl Davis [2]. These researchers have numerically solved the free movement in a square chamber with insulated horizontal walls and vertical walls at two fixed and different temperatures. Also, Nakamura and his colleagues [3] have investigated the effect of temperature difference in creating immersion movements in fluid. In their research, they have predicted changes in fluid flow by using Bozinsk approximation and numerical solution of Navier-Stokes equations and have investigated the rate.

5- References

[1]. Ooi, K. J., Chu, H. S., Bai, P., & Ang, L. K. (2014). Electro-optical graphene plasmonic logic gates. Optics letters, 39(6), 1629-1632.

[2]. Kim, S., Choi, Y. J., Choi, Y., Kang, M. S., & Cho, J. H. (2017). Large-Area Schottky Barrier Transistors Based on Vertically Stacked Graphene–Metal Oxide Heterostructures. Advanced Functional Materials, 27(30), 1700651.

[3]. Tian, M., Hu, Q., Gu, C., Xiong, X., Zhang, Z., Li, X., & Wu, Y. (2020). Tunable 1/f Noise in CVD
Bernal-Stacked Bilayer Graphene Transistors. ACS applied materials & interfaces, 12(15), 17686-17690.

[4]. Wu, Y., Farmer, D. B., Xia, F., & Avouris, P. (2013). Graphene electronics: Materials, devices, and circuits. Proceedings of the IEEE, 101(7), 1620-1637.

[5]. Jiao, L., Wang, X., Diankov, G., Wang, H., & Dai, H. (2010). Facile synthesis of high-quality graphene nanoribbons. Nature nanotechnology, 5(5), 321-325

[6]. Xin, G., Hwang, W., Kim, N., Cho, S. M., & Chae, H. (2010). A graphene sheet exfoliated with microwave irradiation and interlinked by carbon nanotubes for high-performance transparent flexible electrodes.Nanotechnology, 21(40), 405201.

[7]. Nair, R. R., Blake, P., Grigorenko, A. N., Novoselov, K. S., Booth, T. J., Stauber, T., ... & Geim, A. K. (2008). Fine structure constant defines visual transparency of graphene. Science, 320(5881), 1308-1308.

[8]. Geim, A. K., & Kim, P. (2008). Carbon wonderland. Scientific American, 298(4), 90-97.
[9]. Ping, J., Vishnubhotla, R., Vrudhula, A., & Johnson, A. C. (2016). Scalable production of high-sensitivity, label-free DNA biosensors based on back-gated graphene field effect transistors. ACS nano, 10(9), 8700-8704.
[10]. Porada, Z., & Schabowska-Osiowska, E. (2001). Optoelectronic logical system EX-OR. Materials Science and Engineering: B, 86(2), 182-184.
[11]. Jiang, L. H., Wang, F., Liang, R., Wei, Z., Meng, H., Dong, H., ... & Qin, S. (2018). Tunable terahertz filters based on graphene plasmonic all-dielectric metasurfaces. Plasmonics, 13(2), 525-530.
[12]. Wei, Z., Li, X., Yin, J., Huang, R., Liu, Y., Wang, W., ... & Liang, R. (2016). Active plasmonic band-stop filters based on graphene metamaterial at THz wavelengths. Optics express, 24(13), 143414351.
[13]. Du, W., Hao, R., & Li, E. P. (2014). The study of few-layer graphene based Mach– Zehnder modulator. Optics Communications, 323, 49-53.
[14]. Emadi, R., Safian, R., & Nezhad, A. Z. (2016). Theoretical modeling of terahertz pulsed photoconductive antennas based on hot-carriers effect. IEEE Journal of Selected Topics in Quantum Electronics, 23(4), 1-9.
[15]. Jia-Chen Liu, Fu-Li Wang, Jun-Yuan Han, You-Zeng Hao, Yue-De Yang, Jin-Long Xiao, Yong-Zhen Huang, "All-Optical Switching and Multiple Logic Gates Based on Hybrid Square–Rectangular Laser", Lightwave Technology Journal of, vol. 38, no. 6, pp. 1382-1390, 2020.
[16]. Kotb, A. (2016). Simulation of high quality factor all-optical logic gates based on quantum-dot semiconductor optical amplifier at 1 Tb/s. Optik, 127(1), 320-325.
[17]. Elsevier. Welcome to Scopus Preview.
[18]. Goudarzi, K., Mir, A., Chaharmahali, I., & Goudarzi, D. (2016). All-optical XOR and OR logic gates based on line and point defects in 2-D photonic crystal. Optics & Laser Technology, 78, 139-142.
[19]. Jiang, Y. C., Liu, S. B., Zhang, H. F., & Kong, X. K. (2015). Design of ultra-compact all optical half subtracter based on self-collimation in the two-dimensional photonic crystals. Optics Communications, 356, 325-329.
[20]. Rani, P., Fatima, S., Kalra, Y., & Sinha, R. K. (2017). Realization of all optical logic gates using universal NAND gates on photonic crystal platform. Superlattices and Microstructures, 109, 619-625.
[21]. Sharma, P., & Kumar, V. D. (2018). All optical logic gates using hybrid metal insulator metal plasmonic waveguide. IEEE Photonics Technology Letters, 30(10), 959-962.
[22]. Sang, Y., Wu, X., Raja, S. S., Wang, C. Y., Li, H., Ding, Y., ... & Shi, J. (2018). Broadband multifunctional plasmonic logic gates. Advanced Optical Materials, 6(13), 1701368.
[23]. Yarahmadi, M., Moravvej-Farshi, M. K., & Yousefi, L. (2015). Subwavelength graphene-based plasmonic THz switches and logic gates. IEEE Transactions on Terahertz Science and Technology, 5(5), 725-731.
[24]. Wu, X., Tian, J., & Yang, R. (2017). A type of all-optical logic gate based on graphene surface plasmon polaritons. Optics Communications, 403, 185-192.
[25]. Bai, J., Wang, J., Jiang, J., Chen, X., Li, H., Qiu, Y., & Qiang, Z. (2009). Photonic NOT and NOR gates based on a single compact photonic crystal ring resonator. Applied optics, 48(36), 6923-6927.
[26]. Jiang, J., Qiang, Z., Xu, X., & Chen, X. (2011). Analysis of photonic logic gates based on single hexagonal-lattice photonic crystal ring resonator. Journal of Nanophotonics, 5(1), 053519.
[27]. Joannopoulos, J. D., Meade, R. D., & Winn, J. N. (1995). Photonic crystals. Molding the flow of light.
[28]. Nagpal, Y., & Sinha, R. K. (2004). Modeling of photonic band gap waveguide couplers. Microwave and optical technology letters, 43(1), 47-50.
[29]. Jiang, J., Wang, J., Xu, X., Li, J., Chen, X., Qiu, Y., & Qiang, Z. (2010, November). New configuration of photonic logic gates based on single hexagonal-lattice photonic crystal ring resonator. In Optoelectronic Devices and Integration III (Vol. 7847, p. 78470T). International Society for Optics and Photonics.
[30]. Noshad, M., Abbasi, A., Ranjbar, R., & Kheradmand, R. (2012, March). Novel all-optical logic gates based on photonic crystal structure. In Journal of Physics: Conference Series (Vol. 350, No. 1, p. 012007). IOP Publishing.
[31]. Rani, P., Kalra, Y., & Sinha, R. K. (2013). Realization of AND gate in Y shaped photonic crystal waveguide. Optics Communications, 298, 227-231 .
[31]. M. Hayati and G. Karimi, "Short-Channel Effects Improvement of Carbon Nanotube Field Effect Transistors," 2020 (ICEE), IEEE.Index, 2020, pp. 1-6, doi: 10.1109/ICEE50131.2020.9260850.